Polychlorides

International Edition: DOI: 10.1002/anie.201604348
German Edition: DOI: 10.1002/ange.201604348

Structural Proof for the First Dianion of a Polychloride: Investigation of $[Cl_8]^{2-}$

*Robin Brückner, Patrick Pröhm, Anja Wiesner, Simon Steinhauer, Carsten Müller, and Sebastian Riedel**

Dedicated to Prof. Karl O. Christe on occasion of his 80th birthday

Abstract: *The polychloride salt $[CCl(NMe_2)_2]^+_2[Cl_8]^{2-}$ was synthesized and crystallized in the ionic liquid [BMP]OTf. The compound was fully characterized by Raman spectroscopy as well as X-ray single-crystal structure determination, and represents the first example of a polychloride dianion to be described. Detailed gas-phase and solid-state calculations concerning the nature of the bonding situation were also performed.*

A large variety of polyhalides have been synthesized and characterized since the first scientific description of the triiodide anion by Tilden et al. in 1866.[1] Whereas the chemistry of polyiodides is vast and exhibits mono-, di-, tri-, and tetraanions,[2] the variety of polyhalides of the lighter homologues bromine and chlorine is much more limited.[3] For fluorine, only $[F_3]^-$ and recently $[F_5]^-$ were spectroscopically detected in rare-gas matrices.[4] Like all polyhalides, polyiodides also consist of the typical building blocks $[I]^-$, I_2, and $[I_3]^-$, which has led to a growing number of monoanions and also dianions having been synthesized.[5] The first was tetraiodide $[I_4]^{2-}$, which was described almost at the same time as the triiodide.[6] Later on, further dianions, such as $[I_8]^{2-}$[7] and the largest known polyiodide dianion $[I_{18}]^{2-}$ were described. Most of the higher polyiodides have a tendency to form large, complex three-dimensional networks and can, therefore, often be described in different ways, for example, $[I_{10}]^{2-}$ has been described as $[I_5]^-_2$.[8] Such networks, however, can often be observed as well for polyiodides with lower iodine contents.[9] Polybromide dianions on the other hand are quite rare. Only $[Br_4]^{2-}$, $[Br_8]^{2-}$, $[Br_{10}]^{2-}$, $[Br_{20}]^{2-}$, and $[Br_{24}]^{2-}$ have been reported so far.[3] Similar to $[I_4]^{2-}$, $[Br_4]^{2-}$ has an almost linear structure and has been known for more than 50 years.[10] $[Br_{10}]^{2-}$ was synthesized in 1990 and possesses a rectangular structure made up of two parallel $[Br_3]^-$ units bridged by two Br_2 units.[11] The structure of $[Br_{20}]^{2-}$ is very complex and can alternatively be described as $[Br]^-_2(Br_2)_9$.[12] $[Br_{24}]^{2-}$, however, also forms a very complex network structure.[13] The Z-shaped $[Br_8]^{2-}$ exists in three similar structures with different cations (see the Supporting Information).[14–16]

Herein we report the synthesis and full characterization of the first polychloride dianion $[Cl_8]^{2-}$, which is part of the ionic compound tetramethylchloroamidinium octachloride $[CCl(NMe_2)_2]^+_2[Cl_8]^{2-}$. This is—to the best of our knowledge—the first described compound exhibiting a polychloride dianion. Interestingly, the polychloride dianions in this compound can be considered as discrete anions and do not show any tendency to form networks often found in other polyhalide species.[2,3,17] Whereas the equivalent dianions of bromine $[Br_8]^{2-}$ and iodine $[I_8]^{2-}$ exhibit a Z-shape, the $[Cl_8]^{2-}$ dianion presented here has a more linear structure (Figure 1).

The compound was crystallized at −22 °C from a solution of tetramethylchloroamidinium chloride ($[CCl(NMe_2)_2]Cl$) and Cl_2 in *N*-butyl-*N*-methylpyrrolidinium triflate ([BMP]OTf). After the addition of chlorine, the melting point of the mixture drops to below −30 °C. This approach to polyhalide synthesis was first used by Feldmann and coworkers in 2011[12] and also recently by our group.[17] Chlorine shows a high solubility in [BMP]OTf (3.6 wt%, 13.1 mol%),

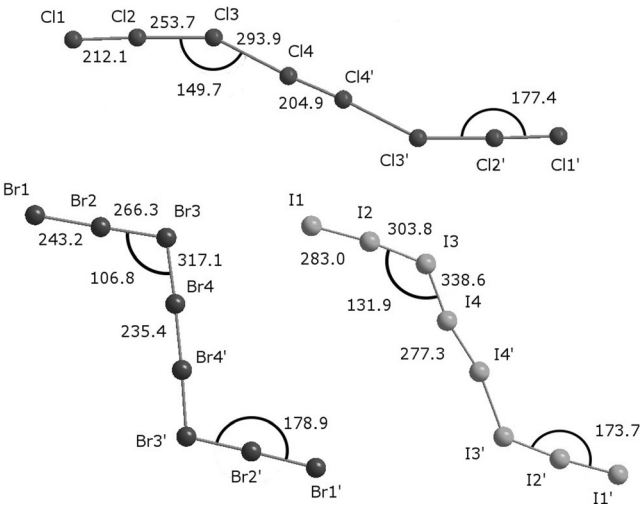

Figure 1. Comparison of the structures of the $[Cl_8]^{2-}$, $[Br_8]^{2-}$, and $[I_8]^{2-}$. For $[Br_8]^{2-}$ and $[I_8]^{2-}$, the structures with the largest (X2-X3-X4) bonding angles were chosen.[15,18]

[*] R. Brückner, P. Pröhm, A. Wiesner, Dr. S. Steinhauer, Prof. S. Riedel
Fachbereich für Biologie, Chemie, Pharmazie
Institut für Chemie und Biochemie—Anorganische Chemie
Fabeckstrasse 34/36, 14195 Berlin (Germany)
E-mail: s.riedel@fu-berlin.de
Dr. C. Müller
Fachbereich für Biologie, Chemie, Pharmazie
Institut für Chemie und Biochemie—Theoretische Chemie
Takustrasse 3, 14195 Berlin (Germany)

Supporting information for this article can be found under: http://dx.doi.org/10.1002/anie.201604348.

which is further enhanced by the addition of $[CCl(NMe_2)_2]Cl$.[17] Storing the mixture for several days at −22 °C led to the formation of small coffin lid shaped crystals.

The salt crystallizes in the monoclinic space group $P2_1/c$. Similar to $[Br_8]^{2-}$ and most of the $[I_8]^{2-}$ structures, $[Cl_8]^{2-}$ is composed of two distorted $[Cl_3]^-$ units which are bridged by a Cl_2 molecule. The bonding angles are 149.7(3)° (Cl2-Cl3-Cl4) and 177.4(4)° (Cl1-Cl2-Cl3; Figure 1). The shortest interanionic distance is 350.5 pm, which corresponds to the sum of the van der Waals radii (350 pm). Therefore, we can speak of discrete $[Cl_8]^{2-}$ dianions, because the interactions between the different anions are very weak. The crystal structure, when viewed along the *b*-axis, shows the anions are arranged in a parallel manner (Figure S1 in the Supporting Information). Observation along the *c*-axis (Figure 2) shows the anions are arranged crosswise, so cavities are formed in which the cations are situated with two different orientations.

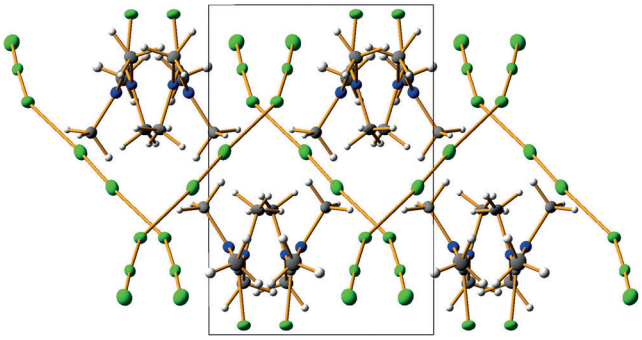

Figure 2. Crystal structure of $[CCl(NMe_2)_2][Cl_8]$ shown along the *c*-axis, exposing the cavities and cations within. C gray, H white, Cl green, N blue.

Interestingly the bond lengths and angles of the $[Cl_8]^{2-}$ anion almost exactly match a motif found in the recently published polychloride network $[Et_4N]_2[(Cl_3)_2{\cdot}Cl_2]$[17] (Table 1). A closer look at the chlorine–chlorine distances Cl1-Cl2 and Cl4-Cl4′ shows they are elongated by only 13 pm and 5 pm, respectively, compared to the bond of free Cl_2 (199 pm).[19] The structure shows considerable $[Cl_2\text{-}Cl^-\text{-}Cl_2\text{-}Cl^-\text{-}Cl_2]$ character. On the other hand, the bond lengths between the inner Cl_2 group and the distorted $[Cl_3]^-$ units ($r_{34} = 293.9(3)$ pm) are considerably longer than the ones within the $[Cl_3]^-$ units ($r_{23} = 253.7(3)$ pm). This bonding situation resembles the one observed in $[PPh_2Cl_2]^+[Cl_3{\cdots}Cl_2]^-$ published by Taraba and Zak in 2003.[20] Thus, the $[Cl_3]^-$ units can be considered as an intermediate between a $[Cl_3]^-$ and a Cl_2 coordinated to a Cl^-. The values of the bonding angles in the crystal structure lead to the assumption that the bonding situation does not, as in $[Br_8]^{2-}$ and $[I_8]^{2-}$, depend to a great extent on σ-hole interactions, which would lead to bonding angles around 90°. This is probably due to the higher electron density around the Cl atoms; for more details see the subsequent discussion.

Table 1: Selected bond lengths and angles in $[Et_4N]_2[(Cl_3)_2{\cdot}Cl_2]$[17] (**4**) and $[CCl(NMe_2)_2]_2[Cl_8]$ (**5**) in the solid state, as well as calculated at the RI-MP2/aug-cc-pVTZ level for an isolated $[Cl_8]^{2-}$ (**6**).

Bond/angle[a]	**4**[17]	**5**	**6**
r_{12}	211.0(3)	212.1(5)	224.5
r_{23}	255.8(3)	253.7(3)	231.4
r_{34}	292.0(3)	293.9(3)	299.1
$r_{44'}$	203.7(4)	204.9(4)	202.6
α_{123}	177.4(2)	177.4(4)	179.6
α_{234}	143.2(3)	149.7(3)	83.4

[a] Bond lengths in pm and angles in °.

Further analysis of the bonding situation was carried out by vibrational spectroscopy (Figure 3). Raman spectroscopy, in particular, is a very powerful technique, as all polyhalide systems show a strong Raman scattering effect. The Raman spectrum of a single crystal of $[CCl(NMe_2)_2]_2[Cl_8]$ shows three

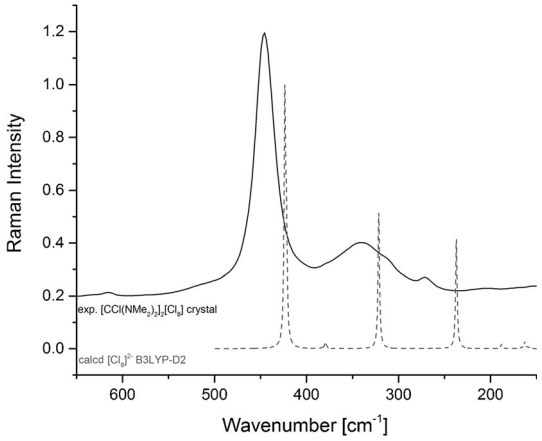

Figure 3. Experimental (——) and calculated (-----) Raman spectrum of the single crystal and the polychloride dianion $[Cl_8]^{2-}$, respectively.

major bands. The intense band at $\tilde{\nu} = 446$ cm^{-1} is assigned to the symmetric stretching vibration of the Cl(4)-Cl(4′) bond and was calculated to appear at $\tilde{\nu} = 424$ cm^{-1}, while the broad band at $\tilde{\nu} = 340$ cm^{-1} is assigned to the stretching vibration of the Cl(1)-Cl(2) bond ($\tilde{\nu}_{calcd} = 322$ cm^{-1}). The small band at $\tilde{\nu} = 271$ cm^{-1} is assigned to the symmetric stretching vibration of the Cl(2)-Cl(3) bond ($\tilde{\nu}_{calcd} = 237$ cm^{-1}). Although these bands show a general shift of approximately 5%, they are in good agreement with our solid-state calculations (B3LYP-D2) and previous investigations of polychlorides, as coordinated Cl_2 molecules often show broad bands around $\tilde{\nu} = 450$ cm^{-1}.[17,20] Additionally, the band at $\tilde{\nu} = 271$ cm^{-1} is where we expect a $[Cl_3]^-$ anion.[21] An analysis of the calculated vibrational modes supports this assignment.

For comparison, the gas-phase structures of $[Cl_8]^{2-}$ and $[Br_8]^{2-}$ were calculated at the B3LYP-D3 and RI-MP2 level. DFT calculations on $[Cl_8]^{2-}$ show spontaneous dissociation, which can be expected because of the well-known Coulomb explosion for dianions in the gas phase.[22] A Z-shaped minimum structure results when the COSMO[23] model ($\varepsilon = 100$) is applied to mimic the stabilizing effect of a surrounding crystal (Figure 4). This structure shows significant similarities to the experimentally found Z-shaped structures of $[Br_8]^{2-}$ and $[I_8]^{2-}$.

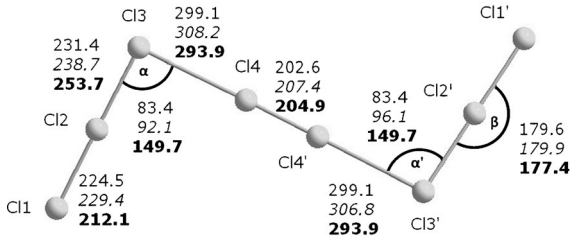

Figure 4. Calculated gas-phase structure of $[Cl_8]^{2-}$. Bond lengths [pm] and angles [°] are given (normal: RI-MP2, italic: B3LYP-D3). For comparison, experimental data are given in bold.

Of course, gas-phase calculations do not include other interactions, for example, packing effects, so bond angles around 90° are preferred because of σ-hole interactions. This is nicely demonstrated by the electrostatic potentials maps around a $[Cl_8]^{2-}$ unit cut out from the experimental crystal structure and for the optimized isolated $[Cl_8]^{2-}$ (Figure 5).

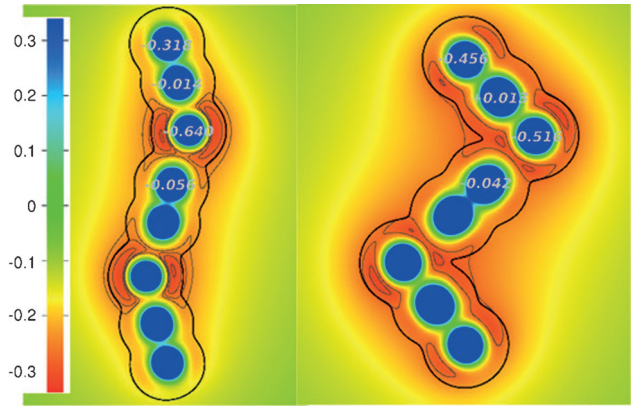

Figure 5. Plot of the electrostatic potential (in a.u.) calculated from a RHF wavefunction of an isolated $[Cl_8]^{2-}$ in the crystal structure (left) and the optimized vacuum structure (B3LYP-D3; right). The thick black line indicates the electron density contour line of 0.001 e bohr^{-3}. Thin gray contours are drawn in the range of −0.34 to −0.24 a.u. at intervals of 0.02 a.u. The numbers in gray are the atomic Mulliken charges calculated from the RHF wavefunction.

The atomic Mulliken charges for the isolated molecules in Figure 5 show that the $[Cl_8]^{2-}$ molecule can indeed be interpreted as an intermediate between Cl_3^--Cl_2-Cl_3^- and Cl_2-Cl^--Cl_2-Cl^--Cl_2. The latter structure is more emphasized in the crystal structure, as observed from the lateral charges of the Cl_3^- units. The electrostatic potentials show that the interactions between the $[Cl_3]^-$ units and the Cl_2 molecule in the crystal are only to a small degree controlled by σ-hole interactions (see above). As seen for the optimized free structure, σ-hole interactions force the molecule into a zig-zag shape with angles of 90°, thus ensuring a good geometric match of the Cl_2-σ-hole and the $[Cl_3]^-$ charge belts, which lead to a stabilization of 16 kJ mol^{-1} compared to the crystal structure.

Two independent periodic calculations were performed, mainly to verify the experimentally recorded spectra (see above): periodic RHF and B3LYP calculations using the Crystal14 program[24] and periodic PAW-PBE calculations using the VASP program.[25] In the former calculation, the cations were replaced by a uniform positive background charge distribution to estimate the packing effects. The purpose of the cations appears to be first of all to prevent the $[Cl_8]^{2-}$ anions from adopting the thermodynamically more stable, σ-hole interaction driven, zig-zag shape. Indeed, the optimized crystal structure differs little from that of the isolated $[Cl_8]^{2-}$ anion in a vacuum. The second purpose of the cations appears to be to prevent the layers of $[Cl_8]^{2-}$ anions from merging due to interlayer σ-hole interactions between two different $[Cl_8]^{2-}$ anions. The latter effect, which is nicely illustrated in yet another electrostatic potential map (Figure 6) of the optimized $[Cl_8]^{2-}$ sublattice, would stabilize the sublattice structure by about 38 kJ mol^{-1} compared to the experimental crystal structure. This leads to the conclusion that the experimentally found chainlike geometry of the $[Cl_8]^{2-}$ anions in the crystal structure of $[CCl(NMe_2)_2]_2[Cl_8]$ is due to packing effects and cannot be ascribed to the generally weak interactions between chlorine atoms.

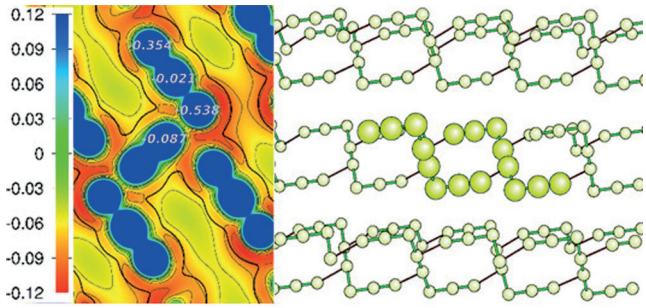

Figure 6. Optimized structure of the periodic $[Cl_8]^{2-}$ sublattice with a uniform charge background (right) and electrostatic potential (in a.u.) calculated from a RHF wavefunction (left). The thick black line indicates the electron density contour line of 0.001 e bohr^{-3}. The thin gray contours are drawn in the range of −0.34 to −0.24 a.u. at intervals of 0.02 a.u. The numbers in gray are the atomic Mulliken charges calculated from the RHF wavefunction.

In the periodic PAW-PBE calculations with plane waves, an optimization of the experimental structure with fixed lattice parameters leads to only slight distortions of the atomic positions. An atoms-in-molecules (AIM) analysis shows that the anions do not seem to form any halogen bonds between one another. The electron density at bond critical points (bcps) between $[Cl_8]^{2-}$ ions is one to two orders of magnitude smaller than the electron density at any bcp within $[Cl_8]^{2-}$ ions. This is very surprising because of the great resemblance between the present structure and **4**, in which halogen–halogen bonding is the driving force. In contrast to the experimental structure, the calculations assume the terminal $[Cl_3]^-$ units to be much more regular. This is consistent with the overestimated bond lengths between the $[Cl_3]^-$ units and the central Cl_2 unit. Thus, the calculated structure describes a $[X_3$-X_2-$X_3]$ adduct, which is also found in specific crystal structures of, for example, $[Br_8]^{2-}$[14,16]l, instead of the $[Cl_2$-Cl^--Cl_2-Cl^--$Cl_2]$ structure found in the crystal.

Table 2 shows no spontaneous dissociation for any of the degradation processes at a DFT level, while at the RI-MP2

Table 2: Calculated bond dissociation energies of polychlorides (in kJ mol^{-1}).[a]

	ΔE (B3LYP)[b]	ΔE (RI-MP2)[b]	ΔE (CCSD(T))
$Cl_8^{2-} \rightarrow Cl_5^- + Cl_3^-$	2.02	−37.53	–
$Cl_8^{2-} \rightarrow Cl_2 + 2\,Cl_3^-$	15.80	−24.95	–
$Cl_8^{2-} \rightarrow 3\,Cl_2 + 2\,Cl^-$	84.59	−145.08	–
$Cl_5^- \rightarrow Cl_2 + Cl_3^-$	13.79	−60.06	40.6[26]
$Cl_3^- \rightarrow Cl_2 + Cl^-$	34.39	12.58	102.9[26]

[a] Basis set: aug-cc-pVTZ. [b] For B3LYP and RI-MP2, the continuous solvent model COSMO was applied ($\varepsilon = 100$).

level, however, decomposition channels are computed to be exothermic, except for the degradation of $[Cl_3]^-$. This inconsistency is probably due to the use of the COSMO[23] solvent model, which is known to overestimate the solvation energies of small fragments.[27] This is confirmed by earlier calculations without the COSMO model, which came to opposite results for the energy values.[26] Nevertheless, these results confirm that polychloride anions are species that depend on very weak interactions.

In conclusion, we report the synthesis and structural characterization of the first polychloride dianion as well as detailed quantum-chemical calculations in the gas phase and solid state. The structure of the compound $[CCl(NMe_2)_2]_2[Cl_8]$ is made up of discrete $[Cl_8]^{2-}$ anions which do not show any tendency to build up networks through halogen bonding. Quantum-chemical calculations confirm that the extraordinary deviation from the Z-like structure of the anions arises from packing effects and not from the poor donor ability of chloride anions.

Experimental Section

All preparative work was carried out using standard Schlenk techniques. The ionic liquid [BMP]OTf was dried under reduced pressure for two days at 50 °C and used without further purification. The Cl_2 gas (purity 2.5) was dried by passing through $CaCl_2$. Oxalyl chloride was used without further purification. Raman spectra were recorded on a Bruker MultiRAM II equipped with a low-temperature Ge detector (1064 nm, 50 mW, resolution 4 cm^{-1}). Single-crystal Raman spectra were measured at −30 °C (1064 nm, 350 mW, resolution 4 cm^{-1}) using a Bruker RamanScope III equipped with a Linkam stage cooling unit.

Tetramethylchloroamidinium chloride was synthesized by literature procedures.[28] Polychloride synthesis: [BMP]OTf (1.32 g, 4.40 mmol) and insoluble tetramethylchloroamidinium chloride (0.377 g, 2.20 mmol) were mixed in a Schlenk tube. Cl_2 was bubbled through the suspension for 5 min, which resulted in the formation of a bright yellow solution. To complete the reaction, Cl_2 addition of was continued for another 5 min. Crystals were obtained by cooling the solution to −22 °C.

Crystal data for $[CCl(NMe_2)_2]_2[Cl_8]$: $C_5H_{12}Cl_5N_2$, $M_r = 277.42$ g mol^{-1}, monoclinic, space group *P21/c*, $a = 1024.77(9)$, $b = 699.08(6)$, $c = 1614.00(11)$ pm, $\beta = 92.845(3)°$, $V = 1154.84(16) \times 10^6$ pm^3, $Z = 4$, $\rho_{calcd} = 1.596$ g cm^{-3}, $F(000) = 564$, $\lambda = 71.073$ pm, $T = 100(2)$ K, absorption coefficient = 1.210 mm^{-1}, absorption correction: multi-scan, $T_{min} = 0.6693$, $T_{max} = 0.7456$. Data for the structure were collected on a Bruker D8 Venture CMOS area detector diffractometer with $Mo_{K\alpha}$ radiation. A single crystal was coated with perfluoroether oil at −30 °C and mounted on a 0.1 mm Micromount. The structure was solved by direct methods in SHELXTL[29] and refined by least squares on weighted F_2 values for all reflections using OLEX2.[30] The final refinements converged at GOF = 1.006, $R1 = 0.0242$, and $wR2 = 0.0550$ for all reflections ($I > 2\sigma(I)$). The hydrogen atoms were included in the refinement in calculated positions by a riding model. The graphical representations were prepared with Diamond.[31] CCDC 1456573 contains the supplementary crystallographic data for this paper. These data can be obtained free of charge from Cambridge Crystallographic Data Centre.

Computational details: Structure optimizations of $[Cl_8]^{2-}$, $[Cl_3]^-$, and Cl_2 were performed at the RI-MP2 level and DFT level using the B3LYP hybrid functional[32] with Grimme's dispersion correction D3[33,34] and the Dunning correlation consistent triple-ζ basis set aug-cc-pVTZ.[35] These calculations were carried out using the Turbomole V7.0.1 program[36] and the COSMO[23] dielectric solvation model with a dielectric constant $\varepsilon = 100$. Minima on the potential energy surface were characterized by calculating harmonic vibrational frequencies. Thermochemistry was provided without any further counterpoise or zero-point energy corrections.

Two periodic DFT calculations were performed, one with and one without counterions. The structure of the periodic $[Cl_8]^{2-}$ sublattice—neglecting counterions—was optimized with the B3LYP density functional and Grimme's[33] dispersion correction D2 as implemented in the Crystal14 program. The more recent D3 scheme[34] is not yet implemented in the Crystal program. An energy-consistent, multi-electron fit, quasirelativistic Stuttgart-Cologne pseudopotential with a chemically inactive [Ne] core[37] was utilized. The valence electrons were represented by a triple-ζ basis set which was derived in a previous investigation of solid chlorine[38] from a (6s6p)/[3s3p] basis set by Dolg,[39] and successfully applied for a similar polychloride solid.[17] (For details about this basis set and its derivation, see the Supporting Information of Ref. [38].) These periodic calculations were performed with the Crystal14 program.[24] An 8 × 8 × 8 Monkhorst-Pack grid was used for *k*-space sampling and truncation criteria for two-electron integrals of 10^{-12}, 10^{-10}, 10^{-10}, 10^{-30}, and 10^{-80} were chosen (thresholds for the overlap of atomic orbitals from pairs of atoms, which determine if Coulomb or exchange integrals are evaluated or not; TOLINTEG, cf. Crystal14 manual). Atomic Mulliken charges and electrostatic potential maps were based on single point restricted Hartree–Fock calculations.

The structure optimization including the cations was carried out with the projector augmented wave (PAW)[40] method and PBE[41] functional, as implemented in the Vienna Ab Initio Simulation Package (VASP).[25] All atomic positions were allowed to relax freely, only cell parameters were fixed to the values obtained from experiment. An energy cut-off of 400 eV and a Monkhorst-Pack *k*-space sampling of 6 × 6 × 6 points were used. Bader analysis was done using the Critic2 program.[42]

Acknowledgements

We gratefully acknowledge the Zentraleinrichtung für Datenverarbeitung (ZEDAT) of the Freie Universität Berlin for computational time. A.W. and C.M. thank the DFG-GRK 1582 "Fluorine as a Key Element" for financial support. We thank Dr. Helmut Beckers for helpful discussions and Lisa Mann for help with Raman microscopy.

Keywords: DFT calculations · halogen–halogen bonding · ionic liquids · polychlorides · solid-state structures

How to cite: *Angew. Chem. Int. Ed.* **2016**, *55*, 10904–10908
Angew. Chem. **2016**, *128*, 11064–11068

[1] W. A. Tilden, *J. Chem. Soc.* **1866**, *19*, 145.
[2] P. H. Svensson, L. Kloo, *Chem. Rev.* **2003**, *103*, 1649–1684.

[3] H. Haller, S. Riedel, *Z. anorg. allg. Chem.* **2014**, *640*, 1281 – 1291.
[4] a) S. Riedel, T. Köchner, X. Wang, L. Andrews, *Inorg. Chem.* **2010**, *49*, 7156 – 7164; b) T. Vent-Schmidt, F. Brosi, J. Metzger, T. Schlöder, X. Wang, L. Andrews, C. Müller, H. Beckers, S. Riedel, *Angew. Chem. Int. Ed.* **2015**, *54*, 8279 – 8283; *Angew. Chem.* **2015**, *127*, 8397 – 8401.
[5] L. Kloo, J. Rosdahl, P. H. Svensson, *Eur. J. Inorg. Chem.* **2002**, 1203 – 1209.
[6] S. M. Jörgensen, *J. Prakt. Chem.* **1870**, *2*, 433 – 458.
[7] E. E. Havinga, K. H. Boswijk, E. H. Wiebenga, *Acta Crystallogr.* **1954**, *7*, 487 – 490.
[8] C. Wieczorrek, *Acta Crystallogr. Sect. C* **2000**, *56*, 1082 – 1084.
[9] C. Horn, M. Scudder, I. Dance, *CrystEngComm* **2001**, *3*, 9.
[10] K. O. Strømme, *Acta Chem. Scand.* **1959**, *13*, 2089 – 2100.
[11] C. W. Cunningham, G. R. Burns, V. McKee, *Inorg. Chim. Acta* **1990**, *167*, 135 – 137.
[12] M. Wolff, J. Meyer, C. Feldmann, *Angew. Chem. Int. Ed.* **2011**, *50*, 4970 – 4973; *Angew. Chem.* **2011**, *123*, 5073 – 5077.
[13] M. E. Easton, A. J. Ward, T. Hudson, P. Turner, A. F. Masters, T. Maschmeyer, *Chem. Eur. J.* **2015**, *21*, 2961 – 2965.
[14] R. Babu, G. Bhargavi, M. V. Rajasekharan, *Eur. J. Inorg. Chem.* **2015**, 4689 – 4698.
[15] K. N. Robertson, P. K. Bakshi, T. S. Cameron, O. Knop, *Z. Anorg. Allg. Chem.* **1997**, *623*, 104 – 114.
[16] M. Wolff, A. Okrut, C. Feldmann, *Inorg. Chem.* **2011**, *50*, 11683 – 11694.
[17] R. Brückner, H. Haller, S. Steinhauer, C. Müller, S. Riedel, *Angew. Chem. Int. Ed.* **2015**, *54*, 15579 – 15583; *Angew. Chem.* **2015**, *127*, 15800 – 15804.
[18] K.-F. Tebbe, B. Freckmann, *Z. Naturforsch. B* **1982**, *37*, 542 – 549.
[19] B. M. Powell, K. M. Heal, B. H. Torrie, *Mol. Phys.* **2006**, *53*, 929 – 939.
[20] J. Taraba, Z. Zak, *Inorg. Chem.* **2003**, *42*, 3591 – 3594.
[21] J. C. Evans, G. Y.-S. Lo, *J. Chem. Phys.* **1966**, *44*, 3638 – 3639.
[22] D. Schröder, *Angew. Chem. Int. Ed.* **2004**, *43*, 1329 – 1331; *Angew. Chem.* **2004**, *116*, 1351 – 1353.
[23] A. Klamt, G. Schüürmann, *J. Chem. Soc. Perkin Trans. 2* **1993**, 799 – 805.
[24] R. Dovesi, V. R. Saunders, C. Roetti, R. Orlando, C. M. Zicovich-Wilson, F. Pascale, B. Civalleri, K. Doll, N. M. Harrison, I. J. Bush, P. D'Arco, M. Llunel, M. Causa, Y. Noël, *Crystal14. User's Manual*, University of Torino, Torino, **2014**.
[25] G. Kresse, J. Hafner, *J. Phys. Condens. Matter* **1994**, *6*, 8245 – 8257.
[26] R. Brückner, H. Haller, M. Ellwanger, S. Riedel, *Chem. Eur. J.* **2012**, *18*, 5741 – 5747.
[27] H. S. Muddana, M. K. Gilson, *J. Chem. Theory Comput.* **2012**, *8*, 2023 – 2033.
[28] V. Štrukil, E. Leksić, E. Mestrović, M. Eckert-Maksić, *Aust. J. Chem.* **2014**, *67*, 1129 – 1133.
[29] G. M. Sheldrick, *Acta Crystallogr.* **2008**, *64*, 112 – 122.
[30] O. V. Dolomanov, L. J. Bourhis, R. J. Gildea, J. A. K. Howard, H. Puschmann, *J. Appl. Crystallogr.* **2009**, *42*, 339 – 341.
[31] K. Brandenburg, *Crystal Impact GbR* **2009**.
[32] a) A. D. Becke, *J. Chem. Phys.* **1993**, *98*, 5648 – 5652; b) C. Lee, W. Yang, R. G. Parr, *Phys. Rev. B* **1988**, *37*, 785 – 789.
[33] S. Grimme, J. Antony, S. Ehrlich, H. Krieg, *J. Chem. Phys.* **2010**, *132*, 154104.
[34] S. Grimme, S. Ehrlich, L. Goerigk, *J. Comput. Chem.* **2011**, *32*, 1456 – 1465.
[35] D. E. Woon, T. H. Dunning, *J. Chem. Phys.* **1993**, *98*, 1358 – 1371.
[36] University of Karlsruhe and Forschungszentrum Karlsruhe GmbH, *TURBOMOLE V7.0.1*, **2015**.
[37] A. Bergner, M. Dolg, W. Küchle, H. Stoll, H. Preuß, *Mol. Phys.* **1993**, *80*, 1431 – 1441.
[38] K. G. Steenbergen, N. Gaston, C. Müller, B. Paulus, *J. Chem. Phys.* **2014**, *141*, 124707.
[39] M. Dolg, *Dissertation*, Universität Stutgart, Stutgart, **1989**.
[40] G. Kresse, D. Joubert, *Phys. Rev. B* **1999**, *59*, 1758 – 1775.
[41] J. P. Perdew, K. Burke, M. Ernzerhof, *Phys. Rev. Lett.* **1996**, *77*, 3865 – 3868.
[42] a) A. Otero-de-la-Roza, M. A. Blanco, A. M. Pendás, V. Luaña, *Comput. Phys. Commun.* **2009**, *180*, 157 – 166; b) A. Otero-de-la-Roza, E. R. Johnson, V. Luaña, *Comput. Phys. Commun.* **2014**, *185*, 1007 – 1018.

Received: May 4, 2016
Published online: August 2, 2016

